Evaluation of Fatigue Lifetime and Elucidation of Fatigue Mechanism in Plasticized Poly(vinyl Chloride) in Terms of Dynamic Viscoelasticity

ATSUSHI TAKAHARA, KENJI YAMADA, TISATO KAJIYAMA, and MOTOWO TAKAYANAGI, *Department of Applied Chemistry, Faculty of Engineering, Kyushu University, Higashi-ku, Fukuoka 812 Japan*

Synopsis

The fatigue behavior of plasticized poly(vinyl chloride) was investigated by means of a tension-compression-type fatigue apparatus. Complex elastic modulus and mechanical loss tangent were obtained continuously with time under the conditions of constant ambient temperature as a function of imposed strain amplitude. Brittle failure was observed under the conditions of low ambient temperatures and small strain amplitudes, or forced convection of air, whereas thermal failure was observed under the conditions of high ambient temperatures, or large strain amplitudes and natural convection of air. In the case of brittle failure, the dynamic storage modulus E' exhibited a maximum and the loss tangent $\tan\delta$ exhibited a minimum on approaching the point of failure. In the case of thermal failure, E' decreased and $\tan\delta$ increased monotonously until the onset of thermal failure. It was found that failure occurs when the effective energy loss reaches a certain magnitude depending on an ambient temperature. The fatigue criterion was represented schematically from a standpoint of self-heating. When the heat generation rate of the specimen under cyclic straining is larger than that of the heat transfer to the surroundings, thermal failure takes place. In this case, the specimen temperature increases up to a limiting constant temperature corresponding to the α-absorption temperature. When the heat generation rate is nearly equal to that of the heat transfer to the surroundings, the specimen temperature does not change appreciably and brittle failure takes place.

INTRODUCTION

Fatigue studies in polymers have been approached along two distinct paths. One has been the mechanical or phenomenological studies on fracture. It has been reported that fatigue failure of many glassy polymers or fibers is induced by the formation of crazes and cracks.[1,2] The relationship between craze or crack propagations and fatigue lifetime was investigated employing samples with induced flaws. This craze and crack propagation method was applied to the rubbers[3,4] and some glassy polymers.[5,6] The formation of cracks was analyzed by the crack nucleation theory for metals developed by Yokobori.[7] This theory, which was modified for polymers by Prevorsek and Lyons,[8,9] can well elucidate the dependences of temperature, frequency, and molecular weight on fatigue lifetime, but it has a disadvantage with respect to the necessity of many parameters and its limited application to polymeric fibers with a high degree of crystallinity.

The other approach has involved molecular considerations, that is, bond strength, orientation, and so on.[10-12] In these studies, the fatigue behavior was discussed in terms of the Zhurkov model on static failure,[13] but the inherent properties of polymeric materials such as viscoelasticity were not considered. In clarifying the fatigue characteristics of polymeric materials, it is important

Journal of Applied Polymer Science, Vol. 25, 597-614 (1980)

0021-8995/80/0025-0597$01.00

to investigate how the viscoelastic behavior of polymeric materials under cyclic deformation influences fatigue behavior. The variation of the dynamic viscoelastic properties during the fatigue process reflects the change in the microstructure of polymeric materials; also, heat due to the damping properties of the specimen is generated during the fatigue process. However, little attempt has been made to elucidate fatigue behavior from a standpoint of viscoelasticity.[14,15]

In this study, the variations of dynamic viscoelastic properties under cyclic straining were investigated under the conditions of various ambient temperatures as a function of imposed strain amplitudes in order to clarify fatigue mechanism and also the fatigue criteria of plasticized poly(vinyl chloride).

EXPERIMENTAL

Sample Preparation for Fatigue Test

The sample used for the fatigue test was poly(vinyl chloride) (p-PVC) Ryuron 700D (degree of polymerization = 1050, Tokuyama Soda Co., Ltd.), plasticized with di-2-ethyl hexyl adipate (DOA). Dioctyl tin maleate was used as stabilizer. The plasticizer and stabilizer contents were 10 and 2 phr, respectively. Figure 1 shows the shape and dimensions of fatigue testing specimen. Plasticized poly(vinyl chloride) was compression molded into films about 6 mm thick in a laboratory press at a temperature of 453 K. The p-PVC plate obtained above was stuffed into the mold of the same shape as the testing piece shown in Figure 1 and pressed for 10 min at 453 K, then quenched by plunging it into ice water. The molded testing pieces were annealed at 373 K for 15 min before fatigue testing.

Fatigue Tester

A tension–compression-type fatigue tester was designed in order to carry out continuous recording of dynamic complex modulus and mechanical loss tangent under the conditions of a constant ambient temperature as a function of imposed strain amplitude.[14] Figure 2 shows the block diagram of the measuring system of stress amplitude and phase difference (time lag between stress and strain signals). The stress and strain amplitudes were measured with strain gauges of the semiconductor type and a DC differential transformer, respectively. Both the stress signal from the strain gauges and the strain signal from the differential transformer were amplified after noises of these signals had been removed by passing them through low-pass filters. The rms (root mean square) value of the amplified stress signal was measured with a digital voltmeter and recorded by a digital printer. The complex elastic modulus can be calculated by dividing

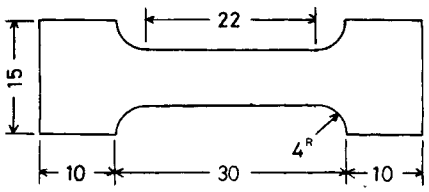

Fig. 1. Dimension of specimen used in fatigue experiment. Thickness of specimen is 5 mm.

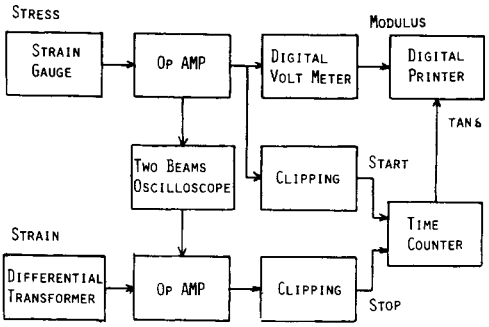

Fig. 2. Block diagram of the measuring system of tension–compression-type fatigue tester.

the stress value by the magnitude of strain amplitude which has been measured before fatigue testing. Both the stress and strain signals were transformed into pulses, and then the phase lag of these pulses was measured with a time counter and recorded by a digital printer. The mechanical loss tangent tan δ can be calculated from the following equation:

$$\tan \delta = \tan \left(2\pi \frac{\Delta t}{T_p} \right)$$

where T_p is a repeating period of cyclic straining of fatigue tester and Δt is a true time lag between stress and strain signals after eliminating the mechanical and electrical time lag. The printing by the digital printer was controlled by a timer. The testing frequency was 6.91 Hz.

The ambient temperature during the fatigue testing was controlled by an air bath equipped with a thermocontroller. During the fatigue testing under forced convection of air, a blower with air blowing at a velocity of 2.7 m^3/min was set near the specimen to remove the generated heat due to the damping properties of the specimen. The surface temperature of the specimen was measured with a thermocouple which was attached to the surface of the specimen by adhesive tape. The output of the thermocouple was recorded by a pen recorder.

Temperature Dependence of Dynamic Viscoelasticity

The temperature dependence of the dynamic viscoelasticity of the specimen, which underwent the same thermal history as the one used for fatigue test, was obtained with a Dynamic Viscoelastometer Rheovibron DDV-IIB (Toyo Baldwin Co., Ltd.).

Observation of Fatigue Fracture Surface

Scanning electron microscope (SEM, JEOL model JSM-50A) was used for morphological observations of the fatigue fracture surface of test specimens.

RESULTS

S–N Curve

Figure 3 shows the S–N curves for the ambient temperatures of 295, 303, 312, and 325 K. The ordinate and abscissa in Figure 3 are initial stress amplitude and lifetime, respectively. Both brittle failure and thermal failure were observed for these testing conditions. In the case of brittle failure, the specimen broke down with crack propagation. In the case of thermal failure, thermal softening occurred in the middle part of the specimen. Brittle failure occurred under conditions of low ambient temperature and small imposed strain amplitude and/or forced convection of air, whereas thermal failure occurred under conditions of high ambient temperature and large imposed strain amplitude. The higher the ambient temperature, the lower the stress amplitude that led to fatigue failure. The slope of the S–N curve in the short lifetime region became smaller with increase in ambient temperature. This fact shows that the lifetime at high ambient temperature is more sensitive to changes in initial stress amplitude. When the specimen was fatigued under forced convection of air to effectively remove generated heat owing to the damping properties of the specimen, brittle failure occurred at relatively large strain amplitude and the lifetime was greatly increased over that of no forced (natural) convection.

Variations of Dynamic Viscoelasticity During the Fatigue Process

Figures 4(a)–4(c) show the variations of dynamic storage modulus E', dynamic loss modulus E'', and mechanical loss tangent tan δ during the fatigue process at an ambient temperature of 295 K as a function of imposed strain amplitude. In the case of imposed strain amplitudes of 1.28 and 1.03% (curves 1 and 2, Fig. 4), E' decreased with increase in the number of cycles, whereas both E'' and tan δ increased monotonously. This viscoelastic behavior is typical of thermal failure. For the imposed strain amplitude of 0.70% (curve 4, Fig. 4), E' increased after reaching a minimum value. Both tan δ and E'' decreased after they temporarily increased. Fracture occurred after E' passed through a maximum and tan δ and E'' reached a minimum. This viscoelastic behavior is typical for brittle failure. For the middle strain amplitude of 0.81% (curve 3, Fig. 4), the variation

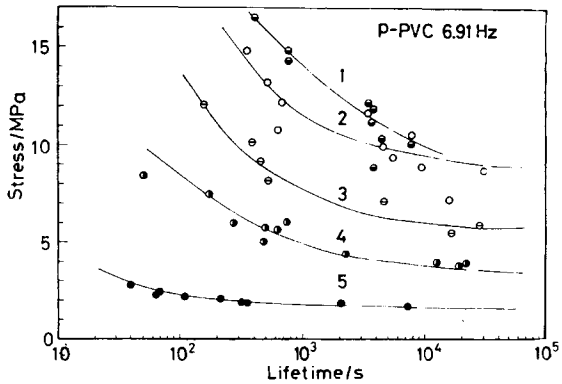

Fig. 3. S–N curves of plasticized poly(vinyl chloride) as function of ambient temperatures of 295 (2 ○), 303 (3 ⊖), 312 (4 ◑), and 325 K (5 ●). 1 ⊖ = 295 K under forced convection.

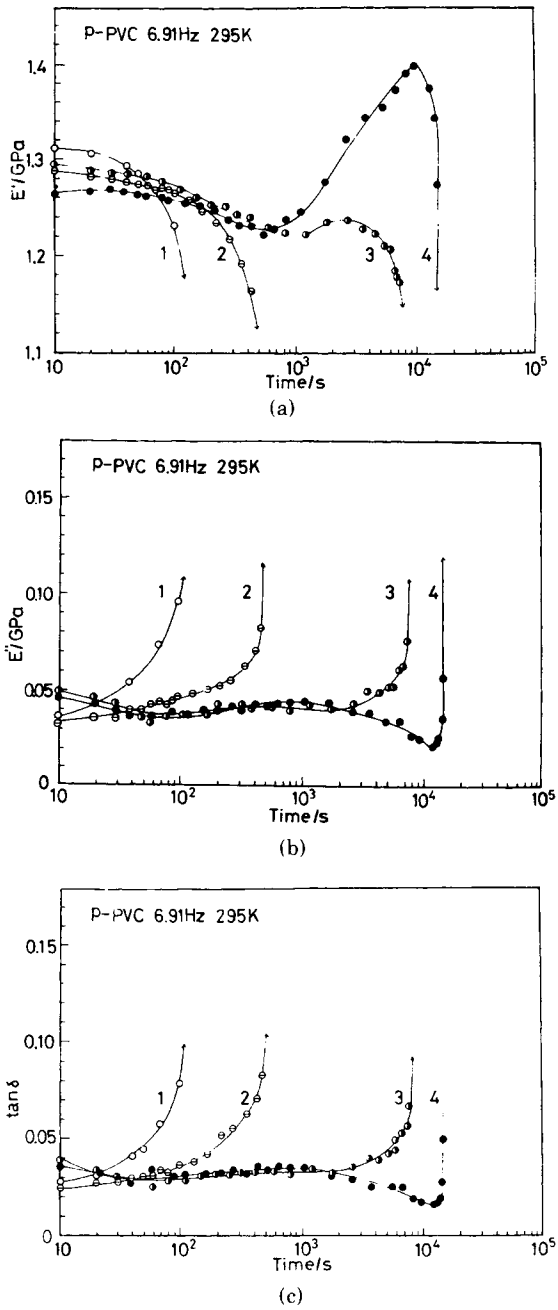

Fig. 4. Variation of E' (a), E'' (b), and tanδ (c) during the fatigue process at ambient temperature of 295 K. Strain amplitude: 1 ○, 1.28%; 2 ⊖, 1.03%; 3 ◑, 0.81%; 4 ●, 0.70%.

of E' during the fatigue process was similar to that for small strain amplitudes of 0.70%, whereas tan δ and E'' increased continuously. This viscoelastic behavior suggests that this imposed strain amplitude of 0.81% leads to an intermediate type of failure between brittle and thermal failures.

Figure 5 shows the variations of dynamic viscoelasticity during the fatigue

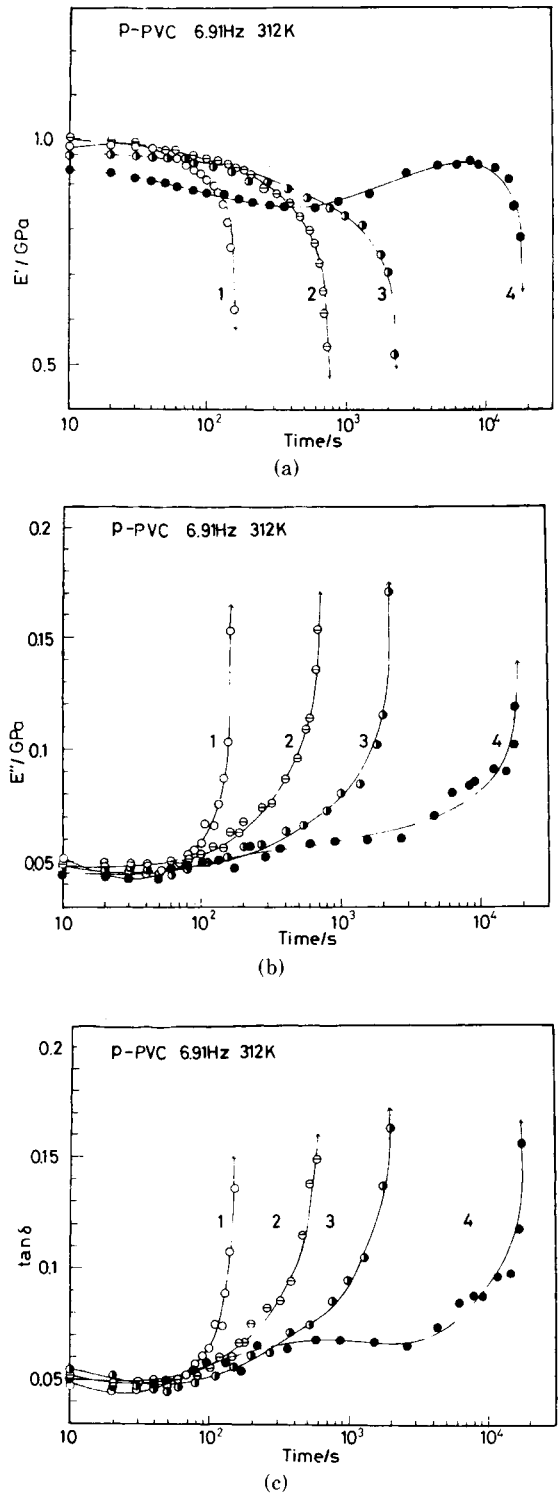

Fig. 5. Variation of E' (a), E'' (b), and tanδ (c) during the fatigue process at ambient temperature of 312 K. Strain amplitude: 1 ○, 0.88%; 2 ◔, 0.61%; 3 ◑, 0.46%; 4 ●, 0.40%.

process at an ambient temperature of 312 K as a function of imposed strain amplitudes. All specimens exhibited typical behavior of thermal failure, and fatigue lifetime became shorter than those for the corresponding strain amplitudes at an ambient temperature of 295 K.

Figure 6 shows the variations of dynamic viscoelasticity during the fatigue process at an ambient temperature of 295 K under forced convection of air as a function of strain amplitudes. In the case of strain amplitudes of 0.70, 0.86, and 1.19% (curves 2, 3, and 4, Fig. 6), a maximum in E' and minima in tan δ and E'' were observed on approaching the point of failure. This behavior corresponds to characteristics of brittle failure as shown in Figure 4. For the strain amplitude of 1.32% (curve 1, Fig. 6), E' continuously decreased with increase in the number of cycles, whereas both tan δ and E'' increased monotonously. Though this viscoelastic behavior is similar to that for thermal failure shown in Figure 4, crack propagation was observed under this testing condition accompanying large plastic deformation. This fact shows that the heat generated during the fatigue process is removed by forced convection of air and thermal failure hardly occurs.

SEM Observation of Fatigue Fracture Surface

Figure 7 shows the SEM micrographs of the fracture surface for the specimen fatigue tested at a strain amplitude of 0.86% and an ambient temperature of 295 K under forced convection of air, for which brittle failure due to crack propagation occurred preferably. The fracture surface is smooth compared with that fractured in liquid nitrogen and shows a fatigue growth pattern resembling a bursting star. The high-magnification SEM micrograph [Fig. 7(b)] shows that each growth band consists of alternating smooth and rough regions. It is speculated that the rough surface might result from the breakdown of craze bands that formed ahead of the propagating crack tips, and the smooth region from brittle fracture crack extension.[16,17] Figure 8 shows the SEM micrographs of the fracture surface for the specimen fatigue tested at a strain amplitude of 0.83% and an ambient temperature of 295 K under forced convection of air. A number of crazes are shown in Figure 8.

DISCUSSION

Viscoelastic Energy Loss Related to Lifetime

Morrow et al.[18] found that the total hysteresis energy dissipated up to failure of some metals was constant under conditions of various ambient temperatures and imposed strain amplitudes. Then the following equation is valid:

$$W_{nv}N_f = \text{Const.} \tag{1}$$

where W_{nv} is the hysteresis energy per cycle and unit volume and N_f is the number of cycles to failure. Opp et al.[19] revealed that eq. (1) could not be applied strictly with respect to the fatigue failure of polymers. Application of eq. (1) for the fatigue failure of polymers must be more precisely considered on fatigue conditions such as imposed strain amplitudes, frequency, ambient temperature, and the heat transfer coefficient. Higuchi and Imai[20] considered the effect of ambient temperature on the fatigue failure of amorphous polymers such as

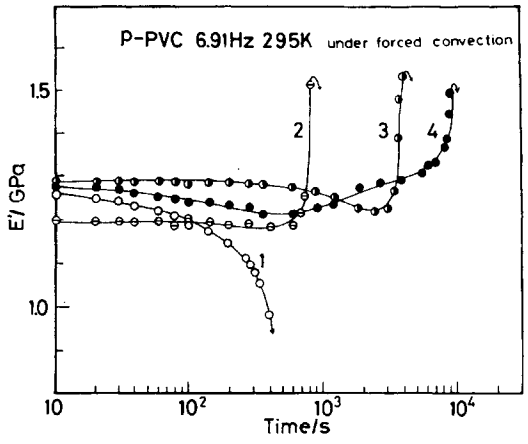

(a)

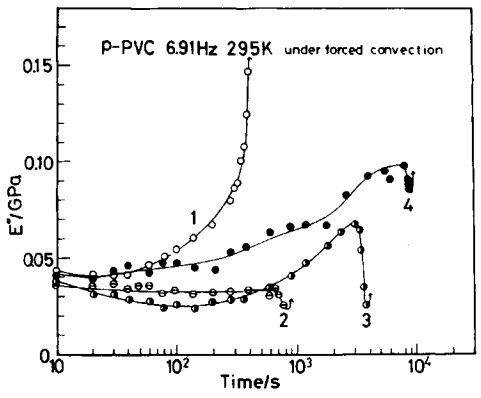

(b)

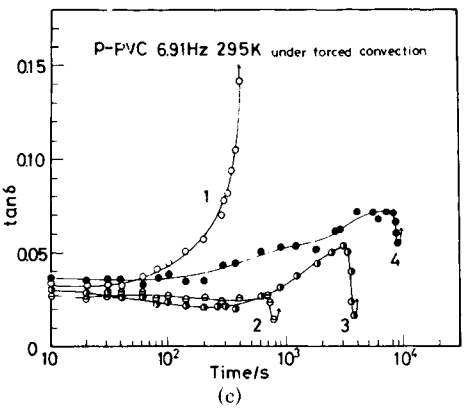

(c)

Fig. 6. Variation of E' (a), E'' (b), and tanδ (c) during the fatigue process at ambient temperature of 295 K under forced convection of air. Strain amplitude: 1 ○, 1.32%; 2 ⊖, 1.19%; 3 ◑, 0.86%; 4 ●, 0.70%.

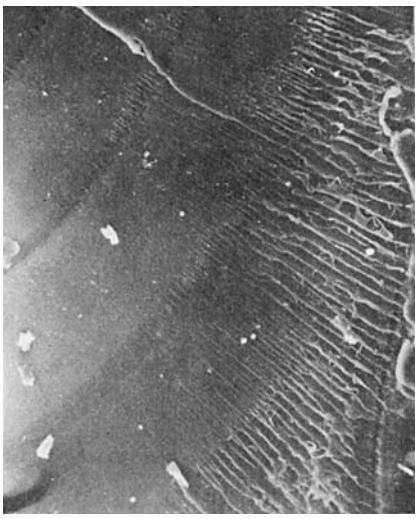

(a)

(b)

Fig. 7. Scanning electron microphotographs of fatigue fracture surface for plasticized poly(vinyl chloride). Strain amplitude was 0.86% and lifetime was 3840 sec.

polycarbonate and poly(methyl methacrylate) and proposed the following equation:

$$(H - a)N_f = C \tag{2}$$

where H is an exothermic coefficient evaluated from the temperature rise of the specimen, N_f is the number of cycles to failure, C is a constant depending on

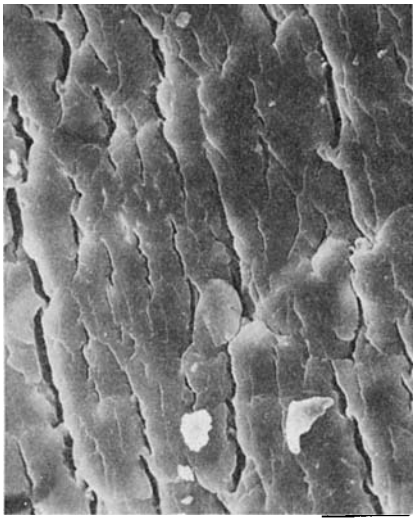

(a)

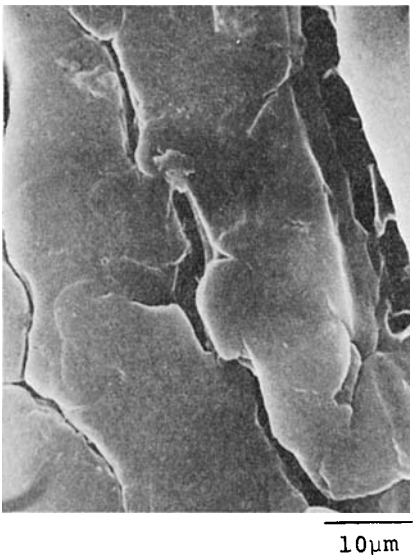

(b)

Fig. 8. Scanning electron microphotographs of fatigue fracture surface for plasticized poly(vinyl chloride). Strain amplitude was 0.83% and lifetime was 2760 sec.

ambient temperature, and a is the exothermic coefficient corresponding to the fatigue limit, which is the inherent constant depending on ambient temperature.

The energy loss of viscoelastic materials under cyclic straining is represented by the following equation:

$$W = \pi f \epsilon^2 E''(T_s) \tag{3}$$

where f, ϵ, and $E''(T_s)$ are frequency, strain amplitude, and dynamic loss modulus

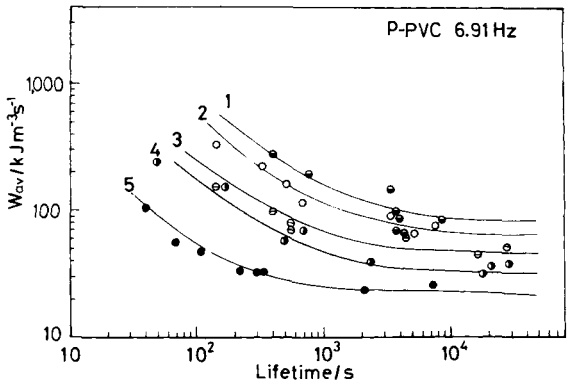

Fig. 9. Relationship between average energy loss W_{av} and lifetime t_f as function of ambient temperatures of 295, 303, 313, and 325 K. See Fig. 3 for legend.

TABLE I
Values of C and W_0 in Eq. (5) for Various Ambient Temperatures

Temperature, K	C, kJ/m^3	W_0, kJ/m^3 s^1
295	60,000	60
295[a]	60,000	87
303	23,000	45
312	17,000	30
325	3,800	25

[a] Under forced convection.

at the specimen temperature T_s, respectively. The average energy loss on cyclic fatigue, W_{av}, is

$$W_{av} = \int_0^{t_f} W\, dt/t_f = \pi f \epsilon^2 \int_0^{t_f} E''(T_s)\, dt/t_f \tag{4}$$

where t_f is the lifetime. Figure 9 shows the relationships between W_{av} and t_f as a function of ambient temperature. The W_{av} values are dependent on lifetime as represented by the following equation:

$$(W_{av} - W_0)t_f = C \tag{5}$$

where W_0 is the energy limit for the generation of fatigue fracture. Table I shows the values of C and W_0 of eq. (5) at various ambient temperatures. As the magnitude of W_0 decreases with increase in ambient temperature, it may be assumed that W_0 is associated with the amount of heat transferred to the surroundings. Figure 10 is a plot of C in eq. (5) against the reciprocal of the ambient temperature, $1/T_0$. It is apparent that C in eq. (5) is represented by an Arrehenius-type equation in the temperature range studied:

$$C = C_{cr} \exp (E_{cr}/RT_0) \tag{6}$$

where E_{cr} is the apparent activation energy, R is the gas constant, and C_{cr} is a constant. From eqs. (5) and (6),

$$(W_{av} - W_0)t_f = C_{cr} \exp (E_{cr}/RT_0) \tag{7}$$

The rate of fatigue process, r, is given by the following equation:

$$r = 1/t_f = (W_{av} - W_0)C_{cr}^{-1} \exp (-E_{cr}/RT_0) \tag{8}$$

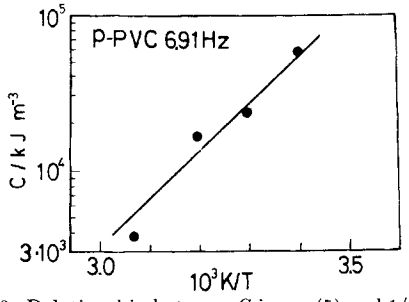

Fig. 10. Relationship between C in eq. (5) and $1/T_0$.

The magnitude of the apparent activation energy for the fatigue process evaluated from the slope of Figure 10 is around 160 kJ/mole. The activation energy of the α-relaxation process for the sample with same thermal history as the one used for fatigue test was evaluated to be around 290 kJ/mole by means of dynamic viscoelastic measurements. Thus, the activation energy of the fatigue process evaluated from eq. (6) is about one-half that for the α-relaxation process of plasticized poly(vinyl chloride). Also, the magnitude of the apparent activation energy E_{cr} of eq. (6) is comparable to that for the breakdown of the C–C bond of plasticized poly(vinyl chloride), 147 kJ/mole.[13]

Relationship Between Strain Amplitude and Lifetime

Coffin[21] derived eq. (9) from the results that the plastic strain ϵ_p depends on the number of cycles to failure, N_f, for low-cycle fatigue of metals:

$$\epsilon_p N_f^{0.5} = \text{Const.} \tag{9}$$

Also, Manson[22] found an analogous relationship with eq. (9) between elastic strain ϵ_e and N_f:

$$\epsilon_e N_f^{0.5} = \text{Const.} \tag{10}$$

Coffin–Manson's equation[23] can be obtained from eqs. (9) and (10):

$$\epsilon t_f^{\,b} = C_{pe} \tag{11}$$

where $\epsilon = \epsilon_p + \epsilon_e$ and both b and C_{pe} are constants. Prevorsek et al.[8,9,24] confirmed that eq. (11) could be applied to the cases for the fatigue failures of various polymeric fibers, such as nylon 6, nylon 66, poly(ethylene terephthalate) fibers, and so on. The magnitudes of b obtained by Prevorsek et al. ranged from 0.08 to 0.13 for these fibers. Figure 11 shows the relationship between strain amplitude and lifetime as a function of ambient temperature. The straight lines were drawn by the least-squares method. The magnitude of b of eq. (11) evaluated from the slope of the straight line is 0.14 under the condition of no forced convection (natural convection). This value is approximately equal to the ones of the polymeric fibers evaluated by Prevorsek et al.[8,9,24]

Figure 12 shows the temperature dependence of C_{pe} of eq. (11). Apparent activation energy evaluated from the slope of this straight line is around 70 kJ/mole. The following equation was obtained for plasticized poly(vinyl chloride) at various ambient temperatures T_0 under no forced convection (natural convection):

$$\epsilon t_f^{0.14} = C_0 \exp\,(E_{pe}/RT_0) \tag{12}$$

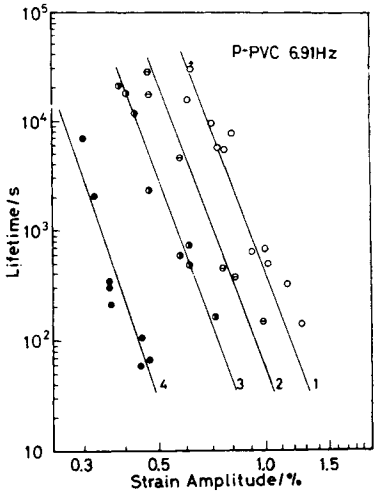

Fig. 11. Relationship between strain amplitude, ϵ, and lifetime t_f as function of ambient temperatures of 295 (1 ○), 303 (2 ⊖), 312 (3 ◑), and 325 K (4 ●).

where C_0 and E_{pe} are a constant and the apparent activation energy, respectively.

Fatigue Failure from the Standpoint of Self-Heating

Figure 13 shows the variations of E', tan δ, and the surface temperature of the specimen, T_s, during thermal failure under the conditions of strain amplitude of 0.83%, ambient temperature of 303 K, and natural convection. Under such conditions of thermal failure, both the surface temperature of the specimen and tan δ increase but E' decreases with increase in fatigue time, resulting in the remarkable variations on approaching the point of failure. In the case of thermal failure of plasticized poly(vinyl chloride), the surface temperature of the specimen rose to 327 K, independently of ambient temperature. This limiting surface temperature is nearly equal to the α-absorption temperature for plasticized poly(vinyl chloride) at 6.91 Hz. Similar results were reported by O'Toole et al.[25,26] Using an IR radiation thermometer, these authors reported that the specimen temperature of PMMA became equal to the α-absorption temperature at the final process of thermal failure.

If a part of energy under cyclic straining is transformed into heat, the rate of

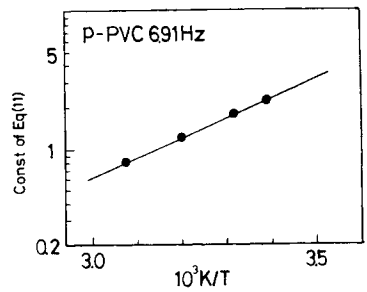

Fig. 12. Relationship between C_{pe} in eq. (11) and $1/T_0$.

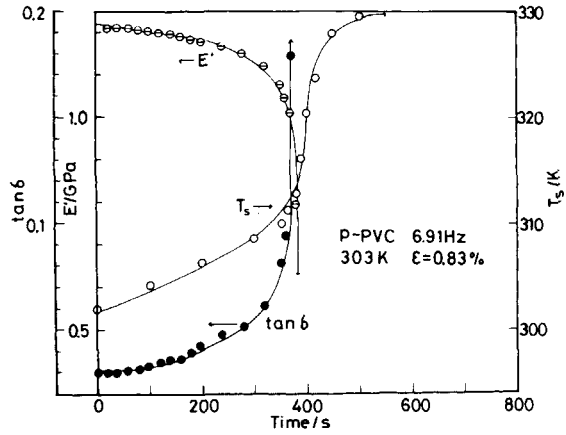

Fig. 13. Variation of E', tanδ, and surface temperature of the specimen, T_s, during thermal failure process under strain amplitude of 0.83% and ambient temperature of 303 K.

self-heating per unit volume, Q_+, can be represented by the following equation:

$$Q_+ = \pi f \epsilon^2 E''(T_s) \tag{13}$$

When the heat generated during the fatigue process raises the specimen temperature without being transferred to the surroundings, the rate of temperature rise of the specimen, dT_s/dt, is

$$\frac{dT_s}{dt} = \frac{1}{\rho c} Q_+ = \frac{\pi f \epsilon^2}{\rho c} E''(T_s) \tag{14}$$

where ρ is the density of the specimen and c is its specific heat. If the amount of heat transferred to the surroundings is proportional to the difference between the surface temperature of the specimen, T_s, and the ambient temperature, T_0, the rate of the heat loss to the surroundings per unit volume, Q_-, is represented by the following equation:

$$Q_- = \kappa(T_s - T_0) \tag{15}$$

where κ is the heat transfer coefficient to the surroundings. From eqs. (13), (14), and (15) the actual rate of the temperature rise of the specimen, dT_s/dt, is given by

$$\frac{dT_s}{dt} = \frac{1}{\rho c}(Q_+ - Q_-) \tag{16}$$

If the temperature of the specimen continues to rise, the following relation should be held[27-29]:

$$Q_+ > Q_-$$

that is,

$$\pi f \epsilon^2 E''(T_s) > \kappa(T_s - T_0) \tag{17}$$

Figure 14 shows the variations of the rate of heat generation, Q_+, and the rate of heat transferred to the surroundings, Q_-, with specimen temperature T_s as

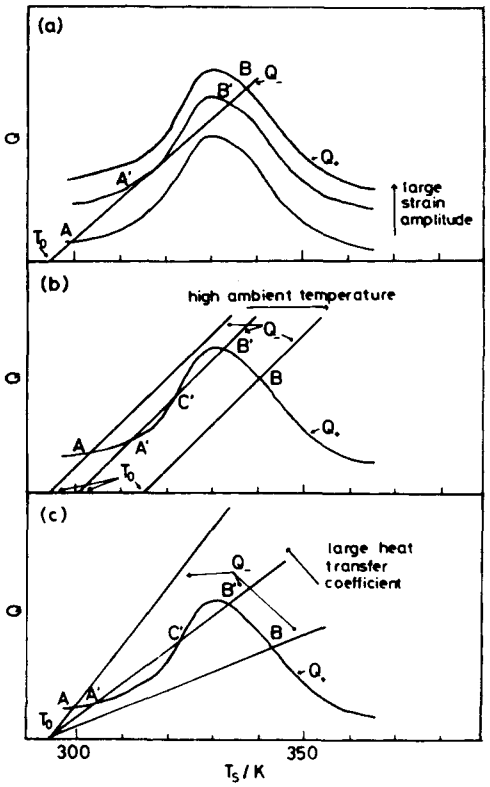

Fig. 14. Variations of heat generation rate Q_+ and heat transfer rate to the surroundings, Q_-, with specimen temperature T_s as function of strain amplitude (a), ambient temperature (b), and heat transfer coefficient to the surroundings (c).

a function of strain amplitude (a), ambient temperature (b), and heat transfer coefficient (c). Since Q_+ is proportional to square of the strain amplitude, ϵ^2, the Q_+ curve for the large strain amplitude is shifted upward, [Fig. 14(a)]. Since Q_- is proportional to the temperature gradient $T_s - T_0$, the Q_- curve is represented as a straight line. A straight line of Q_- shifts along the abscissa for various ambient temperatures [Fig. 14(b)]. According to eq. (15), the slope of the straight line of Q_- is proportional to the magnitude of the heat transfer coefficient κ [Fig. 14(c)]. When Q_- intersects Q_+ at the lower temperature of point A, T_s(A), which is a few degrees higher than the ambient temperature T_0, the specimen temperature rises at the beginning of the fatigue experiment and attains steady state at the specimen temperature $T_s(A)$. The fatigue process proceeds at T_s(A), and finally brittle failure takes place. On the other hand, when Q_- intersects Q_+ at the higher temperature of point B, T_s(B), which is nearly equal to the α-absorption temperature of the specimen, the specimen temperature increases up to the steady-state temperature of T_s(B). This fatigue condition induces thermal failure. When Q_- is tangent to the curve of Q_+ at the lower-temperature region, [point A′ in Fig. 14(a)] and intersects it at a higher temperature, [point B′ in Fig. 14(a)], the transition behavior from brittle failure to thermal failure will be observed. The corresponding fatigue failure behavior is curve 3 of Figure 4 obtained under the conditions of an ambient temperature of 295 K and imposed strain amplitude of 0.81%.

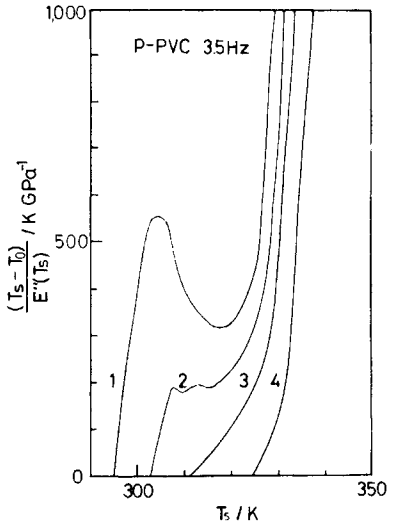

Fig. 15. $(T_s - T_0)/E''(T_s)$ in eq. (18) as function of specimen temperature T_s. Ambient temperature: 1, 295 K; 2, 303 K; 3, 312 K; 4, 325 K.

Brittle failure took place under small imposed strain amplitude and low ambient temperature or large heat transfer coefficient to the surroundings, as shown in Figure 14. Therefore, brittle failure proceeds in a thermal equilibrium state at a temperature below T_s(A). On the other hand, as shown in Figure 14, thermal failure took place under large imposed strain amplitude or high ambient temperature and small heat transfer coefficient to the surroundings. Therefore, thermal failure proceeds in the thermal equilibrium state at a temperature above T_s(B). Since the magnitude of the heat transfer coefficient is proportional to the 0.8th power of the mass velocity of air, κ is larger under forced convection of air. Therefore, even if thermal failure took place without forced convection of air, brittle failure will be occasionally observed with forced convection of air even at relatively large imposed strain amplitudes as previously described.

Equation (17) can be rewritten as follows[30]:

$$\frac{\pi f \epsilon^2}{\kappa} > \frac{T_s - T_0}{E''(T_s)} \tag{18}$$

Figure 15 shows the relationship between $(T_s - T_0)/E''(T_s)$ and the specimen temperature T_s. The magnitudes of $(T_s - T_0)/E''(T_s)$ are calculated from $E''(T)$ obtained by dynamic mechanical measurements for the case of ambient temperatures of 295, 303, 312, and 325 K. Although the temperature dependence of $E''(T_s)$ involves structural changes of the specimen during the fatigue process, we applied the original temperature dependence of $E''(T_s)$ to calculate the right side of eq. (18) for simplicity. The curve $(T_s - T_0)/E''(T_s)$ at an ambient temperature of 295 K exhibits a maximum around 303 K and a minimum around 318 K. When the magnitude of $\pi f \epsilon^2/\kappa$ is smaller than the maximum of the $(T_s - T_0)/E''(T_s)$ curve at around 303 K, the specimen is in thermal equilibrium at a temperature below 303 K and brittle failure takes place. On the other hand, when the magnitude of $\pi f \epsilon^2/\kappa$ is larger than the maximum of the $(T_s - T_0)/E''(T_s)$ curve, the specimen holds the thermal equilibrium around 327 K in which

thermal failure takes place. However, if the heat transfer coefficient increases under forced convection of air, the magnitude of $\pi f\epsilon^2/\kappa$ becomes lower and brittle failure takes place instead of thermal failure. The curves of $(T_s - T_0)/E''(T_s)$ at an ambient temperature of 312 and 325 K no longer exhibit a maximum or a minimum but increase monotonously with surface temperature of the specimen. Such an increase in $(T_s - T_0)/E''(T_s)$ becomes particularly remarkable above 325 K. It is ascertained from Figure 15 that the equilibrium temperature becomes almost constant when the magnitude of $(T_s - T_0)/E''(T_s)$ increases remarkably in the thermal failure region. This phenomenon apparently indicates that the specimen temperature for thermal failure is about 327 K, independent of the ambient temperature.

CONCLUSIONS

Two characteristic types for fatigue failure of plasticized poly(vinyl chloride) have been observed, that is, brittle failure and thermal failure. In the case of brittle failure, the dynamic storage modulus E' exhibits a maximum and the loss tangent tan δ exhibits a minimum on approaching the point of failure. In the case of thermal failure, E' decreases and tan δ increases monotonously from the start of the fatigue testing until failure. The average energy loss during the fatigue process, W_{av}, is dependent on both lifetime t_f and ambient temperature T_0, as represented by the following equation:

$$(W_{av} - W_0)t_f = C_{cr} \exp (E_{cr}/RT_0)$$

where W_0 is the energy loss due to the fatigue limit, C_{cr} is a constant, E_{cr} is the apparent activation energy of the fatigue process, and R is the gas constant. The value of E_{cr} is 160 kJ/mole, which is comparable to that for scission of the C–C bond of poly(vinyl chloride). The relationship between imposed strain amplitude ϵ and t_f for various ambient temperatures can be represented by the following equation:

$$\epsilon \cdot t_f^{0.14} = C_0 \exp (E_{pe}/RT_0)$$

where C_0 is a constant and E_{pe} is the apparent activation energy which was evaluted at 70 kJ/mole.[1]

Under the conditions of large imposed strain amplitude, or high ambient temperature and no forced convection of air (natural convection), the heat generation rate in the specimen is larger than the heat transfer rate to the surroundings. The specimen temperature increases up to a certain temperature corresponding to the α-absorption temperature for plasticized poly(vinyl chloride) and the specimen breaks down in the manner of thermal failure. On the other hand, under the conditions of small strain amplitude and low ambient temperature and/or forced convection of air, that is, a large heat transfer coefficient, the heat generation rate in the specimen is nearly equal to the heat transfer rate to the surroundings at the lower specimen temperature and the specimen breaks down in the manner of brittle failure.

The authors wish to express their sincere thanks to Professor T. Takemura of Kyushu University for his kind guidance in the construction of the tension–compression fatigue tester.

References

1. S. Rabinowitz, A. R. Krause, and P. Beardmore, *J. Mater. Sci.*, **8,** 11 (1973).
2. J. Murray and D. Hull, *Polymer*, **10,** 451 (1969).
3. E. H. Andrews, *Fracture in Polymers*, Oliver & Boyd, London, 1968.
4. A. N. Gent, P. B. Lindley, and A. G. Thomas, *J. Appl. Polym. Sci.*, **8,** 455 (1964).
5. S. L. Kim, M. Skibo, J. A. Mason, and R. Hertzberg, *Polym. Eng. Sci.*, **17,** 194 (1974).
6. N. E. Waters, *J. Mater. Sci.*, **1,** 354 (1966).
7. T. Yokobori, *J. Phys. Soc. Jpn.*, **7,** 44 (1952).
8. D. C. Prevorsek and W. J. Lyons, *J. Appl. Phys.*, **35,** 3152 (1964).
9. D. C. Prevorsek and W. J. Lyons, *Text. Res. J.*, **34,** 881 (1964).
10. V. R. Regel and A. M. Leksovskii, *Mekh. Polim.*, **4,** 70 (1974).
11. V. Zilvar, *J. Macromol. Sci. Phys.*, **5,** 273 (1971).
12. J. L. Weaver and C. L. Beatty, *Polym. Eng. Sci.*, **18,** 1117 (1978).
13. S. N. Zhurkov, *Int. J. Fract. Mech.*, **1,** 311 (1965).
14. C. Nakafuku, S. Taki, and T. Takemura, *Rep. Progr. Polym. Phys. Jpn.*, **15,** 359 (1972).
15. M. Schrager, *J. Polym. Sci. Part A-2*, **8,** 1999 (1970).
16. J. A. Sauer, A. D. Mcmaster, and J. D. Morrow, *J. Macromol. Sci. Phys.*, **12,** 535 (1976).
17. M. L. Owen and R. G. Rose, *J. Mater. Sci.*, **10,** 1711 (1975).
18. C. E. Feltner and J. D. Morrow, *Trans. ASME Ser. D*, **83,** 15 (1961).
19. D. A. Opp, D. W. Skinner, and R. J. Wiktorek, *Polym. Eng. Sci.*, **9,** 121 (1969).
20. M. Higuchi and Y. Imai, *J. Appl. Polym. Sci.*, **14,** 2377 (1970).
21. L. F. Coffin, Jr., *Trans. ASME*, **76,** 931 (1954).
22. S. S. Manson, *Exp. Mech.*, **5,** 193 (1965).
23. P. P. Gills, *Acta Metall.*, **14,** 1673 (1966).
24. D. C. Prevorsek and W. J. Lyons, *Rubber Chem. Technol.*, **44,** 221 (1971).
25. M. N. Ridell, G. P. Koo, and J. L. O'Toole, *Polym. Eng. Sci.*, **6,** 363 (1966).
26. G. P. Koo, M. N. Ridell, and J. L. O'Toole, *Polym. Eng. Sci.*, **7,** 182 (1967).
27. S. B. Ratner and V. I. Korobov, *Mekh. Polim.*, **1**(3), 93 (1965).
28. T. R. Tauchert and S. M. Afzel, *J. Appl. Phys.*, **38,** 4568 (1967).
29. T. R. Tauchert, *Int. J. Eng. Sci.*, **5,** 353 (1967).
30. I. Constable, J. G. Williams, and D. J. Burns, *J. Mech. Eng. Sci.*, **12,** 20 (1970).

Received June 26, 1979
Revised October 5, 1979